Three dimensional nanoparticle trapping enhanced by surface plasmon resonance

Jingzhi Wu and Xiaosong Gan*

Centre for Micro-Photonics, Faculty of Engineering and Industrial Sciences, Swinburne University of Technology, PO Box 218, Hawthorn, VIC-3122, Australia
**xgan@swin.edu.au*

Abstract: We demonstrate a three dimensional nanoparticle trapping approach aided by the surface plasmon resonance of metallic nanostructures. The localized surface plasmon resonance effect provides strong electromagnetic field enhancement, which enables confinement of nanoparticles in the three-dimensional space. Numerical simulations indicate that the plasmonic structure provides approximately two orders of magnitude stronger optical forces for trapping nanoparticles, compared with that without nanostructures. The study of thermal effect of the plasmonic structure shows that the impact of the thermal force is significant, which may determine the outcome of the nanoparticle trapping.

OCIS codes: (350.4855) Optical tweezers or optical manipulation; (240.6680) Surface plasmons; (310.6628) Nanostructures.

References and links

1. K. Dholakia, P. Reece, and M. Gu, "Optical micromanipulation," Chem. Soc. Rev. **37**(1), 42–55 (2008).
2. M. Dienerowitz, M. Mazilu, and K. Dholakia, "Optical manipulation of nanoparticles: a review," J. Nanophoton. **2**(1), 021875 (2008).
3. J. R. Moffitt, Y. R. Chemla, S. B. Smith, and C. Bustamante, "Recent advances in optical tweezers," Annu. Rev. Biochem. **77**(1), 205–228 (2008).
4. W. B. Russel, "Brownian Motion of Small Particles Suspended in Liquids," Annu. Rev. Fluid Mech. **13**(1), 425–455 (1981).
5. M. Gu, J. B. Haumonte, Y. Micheau, J. W. M. Chon, and X. Gan, "Laser trapping and manipulation under focused evanescent wave illumination," Appl. Phys. Lett. **84**(21), 4236–4238 (2004).
6. K. C. Toussaint, M. Liu, M. Pelton, J. Pesic, M. J. Guffey, P. Guyot-Sionnest, and N. F. Scherer, "Plasmon resonance-based optical trapping of single and multiple Au nanoparticles," Opt. Express **15**(19), 12017–12029 (2007).
7. P. Mühlschlegel, H.-J. Eisler, O. J. F. Martin, B. Hecht, and D. W. Pohl, "Resonant optical antennas," Science **308**(5728), 1607–1609 (2005).
8. C. Girard, E. Dujardin, G. Baffou, and R. Quidant, "Shaping and manipulation of light fields with bottom-up plasmonic structures," N. J. Phys. **10**(10), 105016 (2008).
9. W. L. Barnes, A. Dereux, and T. W. Ebbesen, "Surface plasmon subwavelength optics," Nature **424**(6950), 824–830 (2003).
10. W. Zhang, L. Huang, C. Santschi, and O. J. F. Martin, "Trapping and sensing 10 nm metal nanoparticles using plasmonic dipole antennas," Nano Lett. **10**(3), 1006–1011 (2010).
11. A. H. J. Yang, S. D. Moore, B. S. Schmidt, M. Klug, M. Lipson, and D. Erickson, "Optical manipulation of nanoparticles and biomolecules in sub-wavelength slot waveguides," Nature **457**(7225), 71–75 (2009).
12. M. Righini, P. Ghenuche, S. Cherukulappurath, V. Myroshnychenko, F. J. García de Abajo, and R. Quidant, "Nano-optical trapping of Rayleigh particles and Escherichia coli bacteria with resonant optical antennas," Nano Lett. **9**(10), 3387–3391 (2009).
13. A. N. Grigorenko, N. W. Roberts, M. R. Dickinson, and Y. Zhang, "Nanometric optical tweezers based on nanostructured substrates," Nat. Photonics **2**(6), 365–370 (2008).
14. M. L. Juan, R. Gordon, Y. Pang, F. Eftekhari, and R. Quidant, "Self-induced back-action optical trapping of dielectric nanoparticles," Nat. Phys. **5**(12), 915–919 (2009).
15. G. Baffou, R. Quidant, and C. Girard, "Heat generation in plasmonic nanostructures: Influence of morphology," Appl. Phys. Lett. **94**(15), 153109 (2009).
16. G. Baffou, C. Girard, and R. Quidant, "Mapping heat origin in plasmonic structures," Phys. Rev. Lett. **104**(13), 136805 (2010).
17. D. Lapotko, "Optical excitation and detection of vapor bubbles around plasmonic nanoparticles," Opt. Express **17**(4), 2538–2556 (2009).

#137782 - $15.00 USD Received 8 Nov 2010; revised 7 Dec 2010; accepted 8 Dec 2010; published 15 Dec 2010

18. R. Saija, P. Denti, F. Borghese, O. M. Maragò, and M. A. Iatì, "Optical trapping calculations for metal nanoparticles. Comparison with experimental data for Au and Ag spheres," Opt. Express **17**(12), 10231–10241 (2009).
19. H. Ditlbacher, A. Hohenau, D. Wagner, U. Kreibig, M. Rogers, F. Hofer, F. R. Aussenegg, and J. R. Krenn, "Silver nanowires as surface plasmon resonators," Phys. Rev. Lett. **95**(25), 257403 (2005).
20. M. Bora, B. J. Fasenfest, E. M. Behymer, A. S. P. Chang, H. T. Nguyen, J. A. Britten, C. C. Larson, J. W. Chan, R. R. Miles, and T. C. Bond, "Plasmon resonant cavities in vertical nanowire arrays," Nano Lett. **10**(8), 2832–2837 (2010).
21. G. I. Stegeman, R. F. Wallis, and A. A. Maradudin, "Excitation of surface polaritons by end-fire coupling," Opt. Lett. **8**(7), 386–388 (1983).
22. X. Gao, and X. Gan, "Modulation of evanescent focus by localized surface plasmons waveguide," Opt. Express **17**(25), 22726–22734 (2009).
23. R. Piazza, and A. Parola, "Thermophoresis in colloidal suspensions," J. Phys. Condens. Matter **20**(15), 153102 (2008).
24. R. C. S. Joy, and E. S. Schlig, "Thermal properties of very fast transistors," IEEE Trans. Electron. Dev. **17**(8), 586–594 (1970).
25. S. Duhr, and D. Braun, "Why molecules move along a temperature gradient," Proc. Natl. Acad. Sci. U.S.A. **103**(52), 19678–19682 (2006).
26. H.-R. Jiang, H. Wada, N. Yoshinaga, and M. Sano, "Manipulation of colloids by a nonequilibrium depletion force in a temperature gradient," Phys. Rev. Lett. **102**(20), 208301 (2009).
27. M. Braibanti, D. Vigolo, and R. Piazza, "Does thermophoretic mobility depend on particle size?" Phys. Rev. Lett. **100**(10), 108303 (2008).

1. Introduction

The optical manipulation [1] of nanoparticles is becoming increasingly important in the context of nanoscience and nanotechnology [2,3]. However, trapping nanoparticles is considered to be more challenging than trapping micron-sized objects because of the diffraction limit of light and the severe Brownian motion of the nanoparticles [4]. Although increasing laser power can enhance trapping force, the threshold of breakdown poses a limitation on maximum trapping power that can be used [3,5,6]. Alternatively, nanostructures or near field techniques can be utilized to focus light beyond the diffraction limit to increase the trapping potential [5,7,8]. Because of the localized surface plasmons (SP) effect of plasmonic nanostructures [9] which allows strong electromagnetic (EM) field enhancement and confinement, plasmonic trapping for nanoparticles has been studied in the past few years [10–14]. But the plasmonic absorption, one of key issues associated with trapping with nanoplasmonic structures, has not been extensively studied. In most cases, the thermal effect on nanoparticle trapping has been overlooked, because in these cases, less than a few degrees (°C) increase in the temperature field create the illusion that thermal effect may not look so important. Recently, the generation of heat in plasmonic structure and the trapped plasmonic nanoparticles has been investigated [15–18]. It has been demonstrated experimentally that laser induced heating may generate vapor bubbles around plasmonic nanoparticles [17], which significantly affect the trapping of plasmonic nanospheres of Au and Ag [18]. However, the direct impact of heat generation of plasmonic nanostructure on the trapping of nanoparticles has not been understood thoroughly, especially at the power range well below the threshold of the bubble generation.

Different geometries of plasmonic nanostructures have been investigated to study such optical properties as field enhancement and confinement. It has been demonstrated that plasmonic nanowires can be employed as efficient resonant cavities, which is advantageous for subwavelength imaging and plasmonic lasers [19]. Three dimensional subwavelength field confinement has been realized experimentally in vertical nanowires arrays [20]. Here we demonstrate a nanoparticle trapping approach based on a plasmonic structure comprising of two vertically aligned metallic nanorods placed on the substrate. A focused incident light field [21] is employed to excite localized plasmonic resonance of the nanostructure. Plasmonic absorption of the nanoplasmonic structures and its consequent contribution to the temperature variation of the local micro-environment are investigated using the Finite Difference Time Domain (FDTD) method [22] and the thermal conduction model [16]. The thermal force is estimated based on the temperature gradient [23].

#137782 - $15.00 USD Received 8 Nov 2010; revised 7 Dec 2010; accepted 8 Dec 2010; published 15 Dec 2010

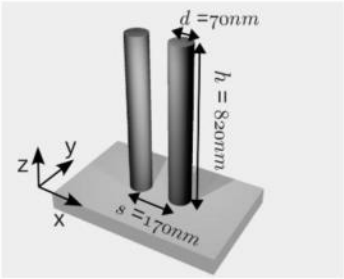

Fig. 1. A schematic diagram of the metallic nanostructure: A linearly polarized (in the *x* direction) laser beam focused by an objective of numerical aperture (NA = 0.5) propagates in the *z* direction from the substrate (n_s = 1.78) into water (n_w = 1.33). The plasmonic structure consists of two vertically aligned silver nanorods immersed in water. The plasmonic rods are 820 *nm* in height *h*, 70 *nm* in diameter *d*, and the centre-to-centre separation *s* is 170 *nm*.

2. Electromagnetic force

2.1 Electromagnetic field enhancement

The configuration of our nanoparticle trapping approach is sketched in Fig. 1. The vertical nanorods show a strong resonance effect when the length *h* matches an odd multiple on quarter plasmon wavelengths [20]. Considering phase shifts occurring on both ends and effective length of the nanorods, we chose the height of the nanorods to be 820 *nm*, with a center-to-center separation of 170 *nm* to support gap modes for the nanoparticles trapping. The two silver nanorods are both 70 *nm* in diameter, vertically aligned and immersed in water (refractive index n_w = 1.33). The laser beam (532 *nm*, linearly polarized in the *x* direction) propagating along *z* through the substrate (refractive index n_s = 1.78) is focused by an objective of numerical aperture (NA = 0.5) with the focal centre at the interface of the substrate and water.

For closer analysis of the plasmonic structure, we performed numerical simulations using the FDTD model [22]. The relative permittivity of the silver rods is described by a classic Drude model $\varepsilon_r = 1 + \left[\omega_p^2 / \left(i\gamma\omega - \omega^2 \right) \right]$, where ω_p = 12120.749 *THz*, γ = 116.10586 *THz*, ω is the angular frequency of the incident light. The FDTD grid size is set to be 4.67 *nm* × 4.67 *nm* × 4.67 *nm*.

Figures 2 (a - c) show intensity distributions in the *xy*, *yz* and *zx* planes, with consideration of the plasmonic nanostructure,while Figs. 2 (d - f) demonstrate the case without presence of the nanostructure. Resonant modes are observed, and the electric field is well confined between the two nanorods with the maximum intensity up to two orders of magnitude stronger. With the strong plasmonic resonance modes, it is noticed that the electric field is not only significantly enhanced in term of field strength, but also better confined three-dimensionally in space. Figure 2 (b) shows the strong evidence that the confinement of the electric field could be less than one quarter of the illuminating wavelength in both *y* and *z* directions. This phenomenon gives clear indication that the use of the plasmonic nanostructures can greatly enhance the optical trapping of nano-particles, which requires a strong electric magnetic field and large field gradient. For the detailed analysis, we studied the optical trapping performance at the resonance peak planes (P1, P3, and P5) and the off-resonance planes (P2 and P4).

#137782 - $15.00 USD Received 8 Nov 2010; revised 7 Dec 2010; accepted 8 Dec 2010; published 15 Dec 2010

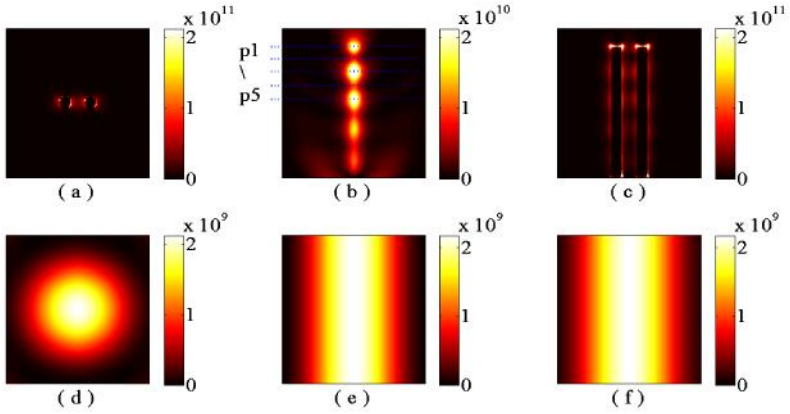

Fig. 2. Comparison of the electric field distributions $|\mathbf{E}|^2$: (a, b, c) with the nanostructure; (d, e, f) without nanostructure; (a, d) in the *xy* plane at a distance of 460 *nm* from the interface, (b, e) in the *yz* plane, (c, f) in the *zx* plane. Dashed lines (P1 ~P5) indicate five positions of resonance maximum and minimum of plasmonic resonance in the structure. All figures are in the size of 930 *nm* × 930 *nm*.

2.2 Electromagnetic force

To quantatively understand the force fields in the plasmonic structure, we calculated the EM force acting on a 30 *nm* nanosphere (refractive index $n = 1.5$) in planes of different distances (P1, P2 and P3 are 820 *nm*, 750 *nm* and 660 *nm*, respectively) from the interface. Figure 3 shows the *x*, *y* components of the EM force (*Fx*, *Fy*) along the *x* and *y* directions in (P1, P2 and P3) planes. For comparison, only the force in the plane P1 for the case without nanostructures is shown, because the *x*, *y* components of EM force remain almost unchanged across P1 – P5 planes (Fig. 2 (e)).

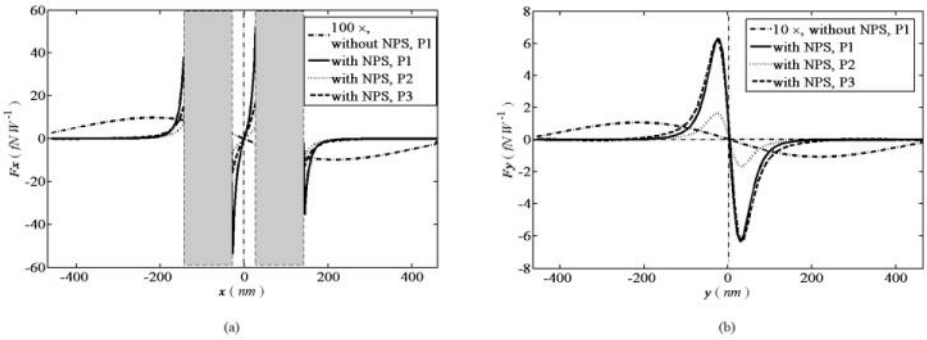

Fig. 3. Comparisons the EM force in transverse dimensions (a) *Fx*, (b) *Fy*. Shaded areas denote the rods.

The calculated plasmonic trapping force profiles (with the nanoplasmonic structures, denoted as with NPS) shown in Fig. 3 suggest stronger trapping force comparing with focused field without the plasmonic structure (denoted as without NPS). Both *Fx* and *Fy* are two orders of magnitude stronger than the forces for the case without the nanoplasmonic structures. This effect is attributed to the strong EM field enhancement and confinement by the nanoplasmonic structure (Fig. 2). With the nanoplasmonic structures, optical trapping field is greatly enhanced, which enables nanoparticle trapping in the gap between the rods. It is noted that the EM force at the resonant planes, e.g. P1 and P3, could be several times as large as that at the non-resonant planes, e.g. P2. For example, *Fy* at the resonance plane P1 is approximately 3 times stronger than the force at the off-resonance plane P2.

#137782 - $15.00 USD Received 8 Nov 2010; revised 7 Dec 2010; accepted 8 Dec 2010; published 15 Dec 2010

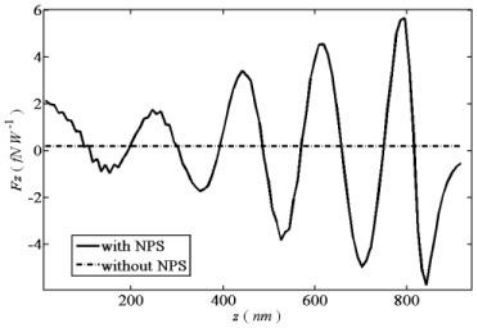

Fig. 4. Comparison of the *z* component of the EM forces as a function of the distance between the nanoparticle and the interface.

In Fig. 4, the longitudinal component of the EM force *Fz* is illustrated. It is noted that with the nanoplasmonic structures, there are several equilibrium trapping positions in the *z* direction, while without the nanoplasmonic structures, there is no equilibrium position for trapping nanoparticle in the *z* direction. It should also be emphasized that longitudinal trapping force is also two orders of magnitude stronger with the presence of the nanoplasmonic structures. Because of plasmonic resonances [9], the electric field enhancement at the edges of the nanostructure is stronger. As a result, the EM force near the upper end of the nanorods is stronger than the force at other positions.

3. Thermal effect

Plasmonic structures can efficiently absorb electromagnetic radiation energy and become the nanosources of heat radiation. Meanwhile, due to the relative low thermal conductivity of dielectric materials compared with metals, thermal gradient will build up in the surrounding media consequently [17]. For nanoparticle trapping in a nano/micro-environment, the thermal gradient produced by the plasmonic structure can create significant disturbance even though the heat generation is in micro-Watts or less.

The heat generation density *q* in a plasmonic structure in an electromagnetic field can be given by

$$q(\mathbf{r}) = \omega\varepsilon_0 \,\mathrm{Im}\{\varepsilon_r\}\left|\mathbf{E}(\mathbf{r})\right|^2 \tag{1}$$

where ε_0 is the permittivity of vacuum, ε_r is the relative permittivity of the plasmonic material, Im denotes the imaginary part, $\mathbf{E}(\mathbf{r})$ is the electric field at position $\mathbf{r}$ which can be calculated using the FDTD simulation [16].

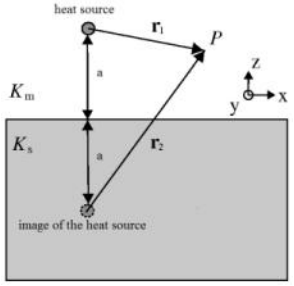

Fig. 5. A heat source image model: a heat source element is located at *z* = a in the medium of thermal conductivity K_m , above the substrate of thermal conductivity K_s.

Assuming that energy dissipated to the environment by the nanostructure is transferred in form of heat conduction. The effect of the substrate on the temperature distribution can be modeled by the heat source image method [24], as shown in Fig. 5. Then, the steady state

#137782 - $15.00 USD Received 8 Nov 2010; revised 7 Dec 2010; accepted 8 Dec 2010; published 15 Dec 2010

temperature distribution within the surrounding medium can be obtained by integration of heat generation density over the plasmonic structure as

$$T(\mathbf{r}) = T_0 + \frac{1}{4\pi K_m}\left(\int_V \frac{q(\mathbf{r})}{r_1} dV - \frac{K_s - K_m}{K_s + K_m}\int_V \frac{q(\mathbf{r})}{r_2} dV\right) \quad (2)$$

where T_0 is the room temperature, r_1, r_2 are the distance from the heat source element dV and its image heat source in the substrate, to the position P, K_m, K_s are the thermal conductivity of the surrounding medium and the substrate respectively (K_m = 0.6 $W\,K^{-1}\,m^{-1}$ and K_s = 1.1 $W\,K^{-1}\,m^{-1}$ is assumed for our simulation).

Due to the presence of thermal gradients, thermophoresis [23,25–27] will occur, which is a phenomenon describes nanoparticle drift in addition to random Brownian motion. Depending on the properties of nanoparticles and surrounding medium, the particles move either towards the cold or the hot zones. Such "thermal forces" have been used for studying colloidal particles or molecules manipulation [25]. For low concentration of nanoparticles, the net force **f** acting on the particle by the solvent due to the present of the temperature gradient can be approximated as linearly proportional to the temperature gradient [23]

$$\mathbf{f} = -\frac{S_T}{\beta}\nabla T \quad (3)$$

where S_T is the Soret coefficient, $\beta = 1/k_B T$, k_B is the Boltzmann constant.

Figure 6 illustrates the heat generation density $q(\mathbf{r})$ and the distribution of the temperature increase δT. The maximum heat generation density q is approximately 0.3 $pW\,nm^{-3}$, which produces maximum temperature increase of approximately 3 K under an input laser power of 10 mW. Because the thermal conductivity of the plasmonic material (silver) is much higher than the surrounding medium (water), the temperature distribution in the nanorods is uniform. The temperature field in the surrounding medium varies with the geometry of the plasmonic structure.

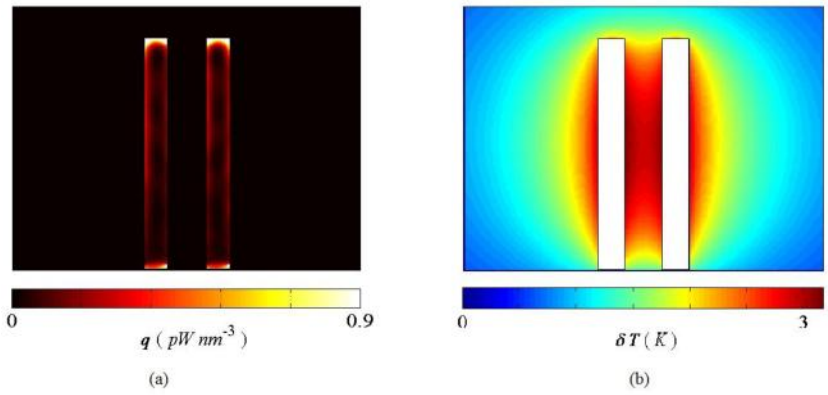

Fig. 6. Thermal absorption of the plasmonic structure. (a) heat generation density, and (b) equilibrium distribution of temperature increase. The incident power is 10 *mW*. All figures are in the size of 930 *nm* × 930 *nm*.

Although the absolute temperature increase of 3 *K* may not look significant, its impact on the local micro-environment can be otherwise. Considering that the 3 *K* temperature increase only occurs in a volume less than one micrometer in all three dimensions, the temperature gradient is rather significant, and hence the thermal force. It is of interest to compare the EM force with the thermal force induced by the temperature gradient. In Fig. 7 we plot the thermal force and the EM force acting on a 30 *nm* (n = 1.5) nanosphere at the resonance (P4) and off-resonance (P5) planes. Taking consideration of the experimental results published earlier

#137782 - $15.00 USD Received 8 Nov 2010; revised 7 Dec 2010; accepted 8 Dec 2010; published 15 Dec 2010

[26,27], we assume that the Soret coefficient $S_T = 2 \times 10^{-4}\ K^{-1}$. The Soret coefficient does not vary significantly if the temperature increase is less than 10 K [27]. However it is noted that S_T strongly is dependent on temperature and particle size, and can even vary from positive to negative at various temperature for different nanoparticle suspensions [23].

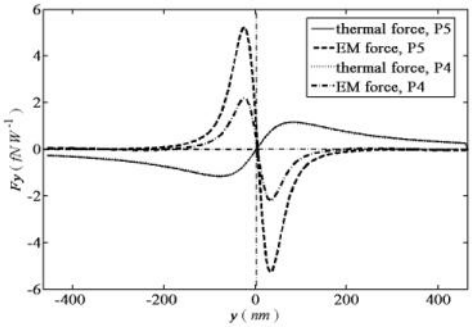

Fig. 7. Comparison of the *y* component of the EM force and of the thermal force at the off-resonance plane P4 and the resonance plane P5. The Soret coefficient S_T used for calculation of is 2×10^{-4} (K^{-1}).

As shown in Fig. 7, the thermal forces decay slower and have a much broader working range than the EM force. Furthermore, according to the experimental results reported earlier [27], the Soret coefficient S_T is negative for aqueous suspensions of 11 *nm* polystyrene spheres in the temperature range of 10 ~40 °C, which leads to the phenomenon that the nanoparticle tends to move towards the hot zone, i.e. towards the plasmonic structure. It is important to notice that the thermal force is comparable to the EM force in terms of the strength. If the Soret coefficient S_T is negative, thermal force can greatly enhance the nanoparticle trapping, since its wide working range makes the capture of nanoparticles easier. However, if the Soret coefficient S_T is positive, it can severely disrupt the optical trapping of nanoparticle.

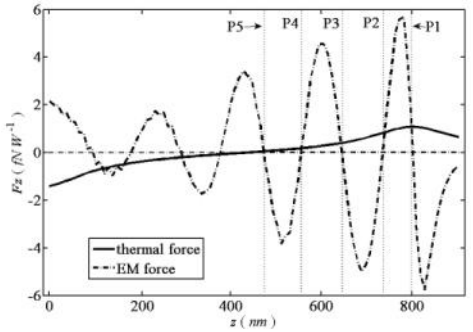

Fig. 8. Comparison of the *z* component of the EM force and of the thermal force as a function of the distance between the nanoparticle and the interface. The vertical dashed lines correspond to the resonance and off-resonance planes shown in Fig. 2 (b). The Soret coefficient S_T used for calculation of thermal force is 2×10^{-4} (K^{-1}).

The *z* components of the thermal force and the EM force are shown in Fig. 8. While the EM force provides multiple trapping equilibrium positions, the thermal force moves the nanoparticle away or towards the center of the plasmonic structure depending upon the Soret coefficient S_T . As the result, nanoparticles can be trapped at positions balancing EM forces with the thermal force, in this case, close to the equilibrium positions of the EM force.

#137782 - $15.00 USD Received 8 Nov 2010; revised 7 Dec 2010; accepted 8 Dec 2010; published 15 Dec 2010

4. Conclusion

In summary, resonances of the plasmonic structure with vertically aligned nanorods give rise to strong electromagnetic field enhancement and confinement three-dimensionally within the gap between the two nanorods. Comparing with the optical trapping without nanorods, the plasmonic structure provides two orders of magnitude stronger optical forces for trapping nanoparticles. It is shown that temperature increase due to the thermal absorption by the nanoplasmonic structure can induce significant temperature gradient in the local micro-environment, which leads to strong thermal forces that comparable to the EM forces in strength. The wide working range of the thermal force makes it a key factor in determining the outcome of trapping nanoparticles.

#137782 - $15.00 USD Received 8 Nov 2010; revised 7 Dec 2010; accepted 8 Dec 2010; published 15 Dec 2010